

Efficient Multi-modal Large Language Models via Visual Token Grouping

Minbin Huang¹ Runhui Huang³ Han Shi² Yimeng Chen⁴ Chuanyang Zheng¹
Xiangguo Sun¹ Xin Jiang² Zhenguo Li² Hong Cheng¹

¹The Chinese University of Hong Kong ²Huawei Noah’s Ark Lab

³The University of Hong Kong ⁴Center of Excellence for Generative AI, KAUST

Abstract

*The development of Multi-modal Large Language Models (MLLMs) enhances Large Language Models (LLMs) with the ability to perceive data formats beyond text, significantly advancing a range of downstream applications, such as visual question answering and image captioning. However, the substantial computational costs associated with processing high-resolution images and videos pose a barrier to their broader adoption. To address this challenge, compressing vision tokens in MLLMs has emerged as a promising approach to reduce inference costs. While existing methods conduct token reduction in the feature alignment phase. In this paper, we introduce *VisToG*, a novel grouping mechanism that leverages the capabilities of pre-trained vision encoders to group similar image segments without the need for segmentation masks. Specifically, we concatenate semantic tokens to represent image semantic segments after the linear projection layer before feeding into the vision encoder. Besides, with the isolated attention we adopt, *VisToG* can identify and eliminate redundant visual tokens utilizing the prior knowledge in the pre-trained vision encoder, which effectively reduces computational demands. Extensive experiments demonstrate the effectiveness of *VisToG*, maintaining 98.1% of the original performance while achieving a reduction of over 27% inference time.*

1. Introduction

The advent of Large Language Models (LLMs) [1, 2, 24, 36] has transformed the landscape of natural language processing (NLP), driving unprecedented advancements across a wide array of tasks, including text generation, sentiment analysis, and machine translation. These models have demonstrated remarkable capabilities in understanding and generating human-like language, setting new benchmarks in various NLP applications. However, as the demand grows for systems capable of handling diverse data types beyond text, the need to integrate information from other

modalities, such as vision, has become increasingly evident. This demand has spurred significant research interest in Multi-modal Large Language Models (MLLMs) [2, 17, 36], which represent a natural extension of LLMs. By incorporating both visual and textual modalities, MLLMs have emerged as a powerful paradigm, capable of achieving superior performance in tasks requiring cross-modal understanding. These tasks include but are not limited to, visual question answering, image captioning, and multi-modal dialogue systems, demonstrating the potential of MLLMs. The synergy between modalities in MLLMs not only enhances their performance but also opens new avenues for innovation in multi-modal AI research and applications. However, the remarkable capabilities of these models come with substantial computational costs, particularly during the inference phase. This computational burden is exacerbated when encountering multi-modal inputs leading to a long input sequence, such as high-resolution images or videos. This limits their practical deployment in resource-constrained environments.

Typically, LLM costs the most for the MLLM computation because of the model size difference compared with the visual encoder and visual connector. For example, the widely used ViT-L [20] only has 0.3B parameters while the language encoder typically has 7B or 13B parameters [8]. Therefore, towards building an effective MLLM, current works focus on reducing the image tokens fed to the LLMs. Various approaches have been applied to serve this purpose. Main stream method includes training-free and finetuning. Training-free methods typically utilize the off-the-shelf pre-trained MLLMs and prune the visual tokens according to the attention in the transformer layers in LLMs [7]. While the training-free method is plug-and-play, their performance is far from satisfying and they are often ineffective when applied to training because the in-training attention scores are unstable. Finetuning methods perform visual token reduction via operations on the image feature produced by the visual encoder, such as Adaptive Average Pooling [30], convolution block or deformable attention block as visual abstractor [5]. However, these methods all

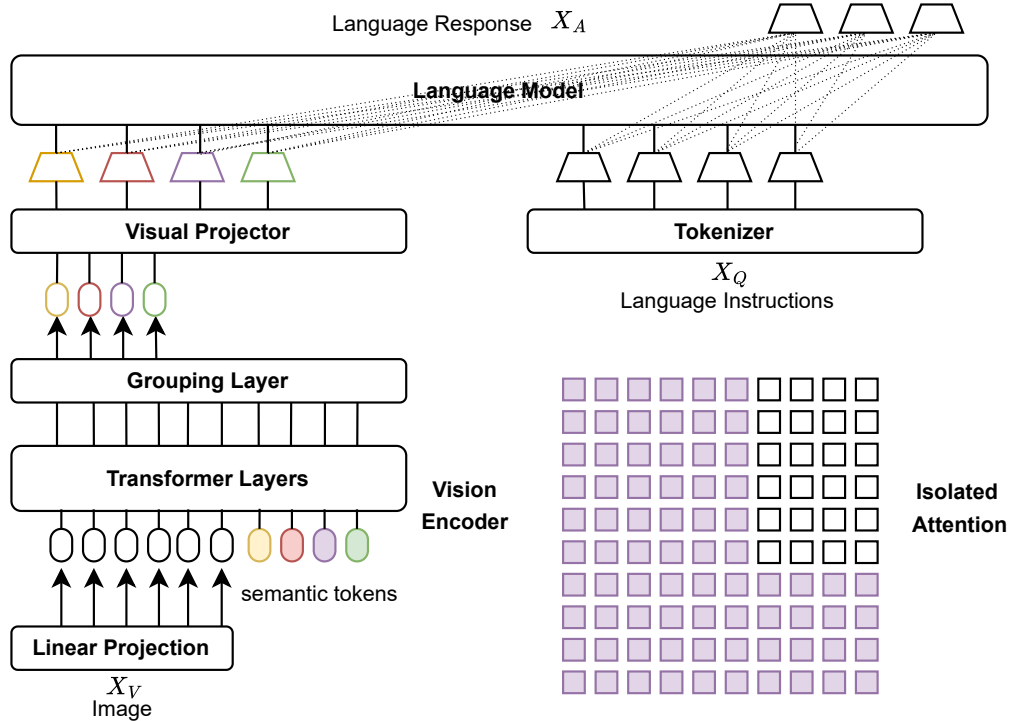


Figure 1. Overview of our proposed VisToG. Semantic tokens are concatenated with the image patch tokens after linear projection and fed into the pre-trained vision encoder. Before the visual projector to LLM, a grouping layer is applied to group similar image segment tokens into semantically abstraction tokens of image. Besides, isolated attention is applied to ensure a better abstraction.

conduct visual token reduction on the image features after feeding into the visual encoder, while leaving the potential of the pre-trained visual encoder not fully explored.

We observe that randomly chosen image tokens can serve as a strong baseline, indicating the redundancy of the image tokens for a certain semantic group. Further, if we deliberately modify the image tokens distribution following prior knowledge from humans, the performance can be greatly improved. Specifically, the sampled tokens covered all semantic segments of the image. Motivated by this, we propose a novel visual token grouping mechanism aimed at reducing the inference costs of MLLMs by exploring the potential of the pre-trained vision encoder to inject prior knowledge, and hence reduce the redundant token while preserving all semantic groups. Our approach leverages the inherent structure and redundancy present in visual data to condense the visual token representation while minimally sacrificing performance. By intelligently grouping visual tokens, we can significantly decrease the number of tokens processed by the model, thereby reducing computational overhead and accelerating inference times.

The main contributions are summarized as follows:

- We propose a novel grouping mechanism VisToG utilizing the pre-trained vision encoder to reduce image tokens sent to the LLMs.
- Extensive experiments prove the effectiveness of VisToG reducing over 27% inference time while maintaining 98.1% of the original performance.

2. Related Work

2.1. Multi-modal Large Language Models

The success of Large Language Models (LLMs) has advanced various applications in natural language processing. Its strong instruction-following ability and generalization power across tasks drive the researchers to build a multi-modal counterpart. GPT-4V from OpenAI has proven the potential of how a Multi-modal Large Language Model (MLLM) can do [29], including but not limited to empowering the Text-to-Image Generation models by recaptioning the training set [3, 15]. Researchers have put efforts to reimplement MLLMs similar to GPT-4V. The core design lies in how to connect the pre-trained visual encoder and the LLM. Resampler [2] and Q-Former [9, 13, 34] em-

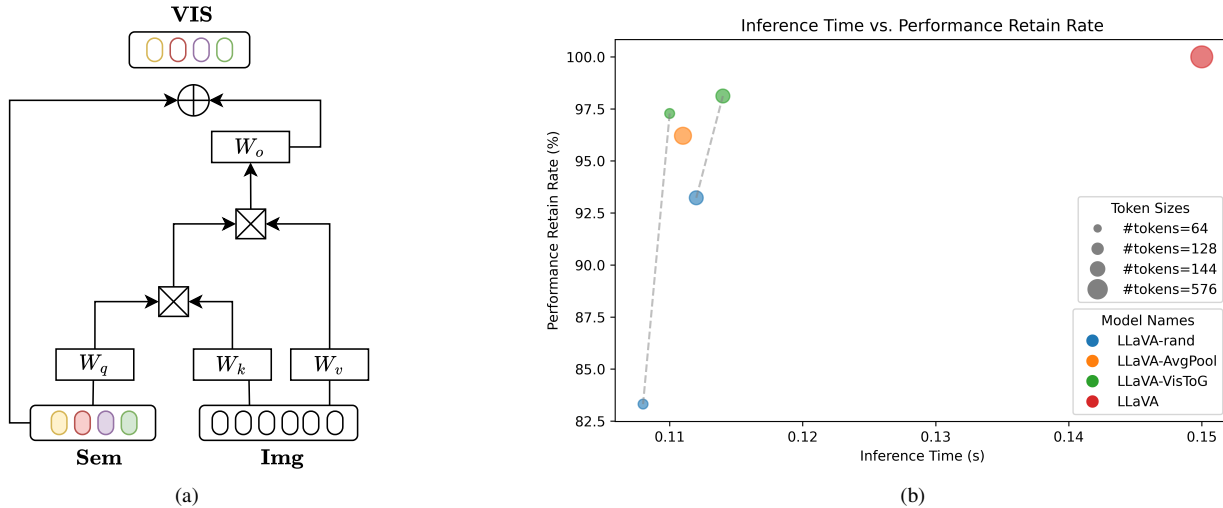


Figure 2. (a) Structure of the grouping layer. (b) Comparison of Inference time and Average Performance between different models.

employs learnable queries to represent visual tokens and force extracting the most relevant visual information from visual features by cross-attention layers. These approaches bridge visual and textual modalities, achieving significant advancements. Text-aligned visual encoders such as CLIP and SigLIP [20, 33] are also key components that contribute to the success of MLLMs, and many works [22, 23, 26] have tried to improve them. To make the alignment between visual encoders and LLMs more effective and efficient, LLaVA [17] uses a single projection layer to conduct the alignment. With a meticulously curated instruction-tuning dataset, it achieves remarkable performance, rivaling models trained on extremely large-scale datasets, yet it requires only a manageable training cost. The reduction in substantial training expenses greatly benefits the MLLM community.

2.2. Efficient inference for LLM/MLLM

The auto-regressive nature of LLMs poses a great challenge to the deployment of LLMs. The quadratic complexity of computing the attention makes the generation process much slower when the input token is longer. StreamingLLM [27] and FastGen [11] prune the redundant attention computation to simplify the computation. Despite their success, they are designed for the single-modal LLM and have not proven successful when it comes to scenarios involving tokens from other modalities. For improving the efficiency of MLLMs, various works [13, 34, 36] adopt Q-Former to map the images to fixed-length tokens. In the meantime, many works try to train smaller MLLMs with smaller backbone [32, 35] to handle the scenario with less computational resources, MoE-LLaVA [16] incorporates a Mixture of Experts to address model sparsity, enhancing efficiency and performance. Another line of research tries to reduce

the number of visual tokens while keeping the backbone of LLM unchanged. Since LLMs contribute most to the computation, the number of input tokens to the LLM becomes the bottleneck of the inference cost. Various works [4, 6] have put effort into increasing the throughput for the vision encoder. DeCo [30] employs 2D adaptive average pooling to down-sample the visual tokens at the patch level. Honeybee [5] proposes to use ResNet Block and deformable attention to conduct the abstraction of the vision tokens. VoCo-LLaMA [31] compress the vision tokens using the LLMs and leverage the attention distillation to let LLMs restore information from the specially defined VoCo tokens instead of the whole image tokens.

3. Method

In this section, we first recap how a typical MLLM works and then introduce VisToG, an innovative approach for efficient visual token grouping in MLLMs. VisToG introduces a novel grouping mechanism that leverages off-the-shelf pre-trained Vision Transformers to cluster similar image segments into semantically related concepts. By doing so, it effectively eliminates the need to encode redundant vision tokens, thereby optimizing computational efficiency.

3.1. Recap of Multi-modal Large Language Models

MLLMs aim to develop a powerful model capable of generating responses that follow the instructions given for multi-modal inputs, including visual and textual data. MLLMs are typically composed of three core components: 1) Visual Encoder E_v : it converts an input image $I \in \mathbb{R}^{H \times W \times 3}$ into a set of distinctive visual embeddings $I_v \in \mathbb{R}^{N \times C}$. CLIP-ViT-L/14 with patch size 14 are widely adopted as the visual encoder due to their language-aligned pretrained

nature, $N = HW/P^2$ denotes the number of visual embeddings. 2) Visual Projector E_p , parametrized by W , which is typically a multi-layer perceptron: this component translates visual embedding I_v into the visual token T_v in the textual embedding space T with an appropriate dimension for the subsequent language model. This part substantially serves as a tokenizer for the input image 3) Large Lanugae Model E_l , parameterized by ϕ : it takes in both visual token T_v and textual token T_t , and produces an appropriate response auto-regressively. For a sequence of responses with length L , we compute the probability of the target answers T_a by

$$p(T_a|T_v, T_t) = \prod_{i=1}^L p_\phi(t_i|T_v, T_{t,<i}, T_{a,<i}), \quad (1)$$

In this framework, the computation burden lies in the LLM with many more parameters than the other components. Therefore, the number of input tokens influences most to the overall efficiency. Therefore, compressing visual tokens becomes the most popular approach to building an efficient MLLM.

3.2. Grouping Layer

To reduce the number of image tokens sent to the LLMs while minimizing the performance loss. Building upon the design in [28], we propose to leverage the capabilities of the pre-trained Vision Encoders. We add several learnable semantic tokens $\{\mathbf{Sem}_i\}_{i=1}^N$ before the transformer layer of ViT and concat it with the image segments $\{\mathbf{Img}_i\}_{i=1}^M$ after the linear projection, where N and M represents the number of semantic groups and original image segments tokens. The Grouping Block takes the learned semantic tokens and image segment tokens as input and merges all the segment tokens that are assigned to the same semantic components into a single new image segment, based on similarity in the embedding space. To be more specific, we compute the similarity matrix \mathbf{A} between the semantic tokens $\{\mathbf{Sem}_i\}_{i=1}^N$ and image segments tokens $\{\mathbf{Img}_i\}_{i=1}^M$ through a Gumbel-Softmax operation computed over semantic tokens as

$$\mathbf{A}_{i,j} = \frac{\exp(W_q \mathbf{Sem}_i \cdot W_k \mathbf{Img}_j + \gamma_i)}{\sum_{k=1}^N \exp(W_q \mathbf{Sem}_k \cdot W_k \mathbf{Img}_j + \gamma_k)} \quad (2)$$

where W_q and W_k are the weights of the learned linear projections for the semantic tokens and image segment tokens respectively and $\{\gamma_i\}$ are i.i.d random samples drawn from the Gumbel (0,1) distribution. Afterward, we compute the semantic group to assign image segment tokens to by taking the one-hot operation of its argmax over all groups. Since the one-hot assignment operation via argmax is non-differentiable, we adopt the straight-through trick in [25] to

compute the assignment matrix as

$$\hat{\mathbf{A}} = \text{one-hot}(\mathbf{A}_{\text{argmax}}) + \mathbf{A} - \text{sg}(\mathbf{A}) \quad (3)$$

where sg is the stop gradient operator. After assigning the image segment tokens to different semantic groups, we merge the embedding of all the tokens belonging to the same semantic group to form a new image token. For each new image token \mathbf{VIS}_i , it is a weighted sum of the image segment tokens assigned to a semantic group, which is computed as

$$\mathbf{VIS}_i = \mathbf{Sem}_i + W_o \frac{\sum_{j=1}^M \hat{\mathbf{A}}_{i,j} W_v \mathbf{Img}_j}{\sum_{j=1}^M \hat{\mathbf{A}}_{i,j} W_v} \quad (4)$$

where W_v and W_o are the learned weights to project the merged features. The structure of the grouping layer is illustrated in Fig. 2

3.3. Isolated attention

To fully leverage the potential of the pre-trained vision encoder, it's crucial to mitigate the impact of the newly introduced semantic tokens, denoted as \mathbf{Sem} , on the original image segment tokens. This ensures that the integrity of the original image representations remains intact. To achieve this, we implement a technique called isolated attention, which prevents the original image segment tokens from interacting directly with the newly added semantic tokens, thereby preserving their original characteristics.

More specifically, let the attention mask M be a matrix defined as $M \in \mathbb{R}^{(M+N) \times (M+N)}$, where each element $M_{i,j}$ represents whether token i can attend to token j . If $M_{i,j} = \text{True}$, token i is allowed to attend to token j , and if $M_{i,j} = \text{False}$, attention is blocked between the two tokens. The isolated attention mechanism is then formally defined as follows:

$$M_{ij} = \begin{cases} \text{False}, & \text{if } i \in \mathbf{Img} \text{ and } j \in \mathbf{Sem}, \\ \text{True}, & \text{otherwise.} \end{cases} \quad (5)$$

This attention mask prevents the original image tokens \mathbf{Img} from attending to the semantic tokens \mathbf{Sem} , while allowing other interactions to proceed normally. Consequently, this design ensures that the output of the original image segment tokens remains unchanged despite the addition of the semantic tokens. By isolating the attention in this way, the original image tokens are preserved as they were before the introduction of the semantic tokens, maintaining the image's core representation.

On the other hand, the semantic tokens \mathbf{Sem} can still learn to aggregate the image features derived from the pre-trained visual encoder into semantically meaningful regions

that align with the provided instruction or task. This approach allows the semantic tokens to specialize in creating groupings of image features without disrupting the original token representations.

We further conduct a series of ablation studies on the attention mask configuration to validate the effectiveness of this isolated attention mechanism compared to using full attention, as detailed in Sec.4. These experiments demonstrate the importance of this isolation in retaining the fidelity of the image representations while allowing the semantic tokens to perform their intended role.

3.4. Instruction-aware Visual Token Grouping

Let ϕ denote the Large Language Model (LLM), W denote the lightweight visual connector, which typically takes the form of a multi-layer perceptron (MLP), and G represent the grouping layer. These components together form the foundation of our method for visual token grouping within an LLM-based framework. To effectively train the proposed VisToG to perform this task, we carefully design a two-stage training pipeline that ensures robust feature alignment and instruction-aware token grouping.

Stage 1: Pre-training for Feature Alignment The goal of the first stage is to align the image features with the LLM by training an image tokenizer that maps visual inputs into a form compatible with the LLM. Since the pre-training phase operates on an image-caption dataset, the grouping mechanism is not yet emphasized during this stage, as the focus is primarily on aligning the visual representation with the caption, which serves as the natural language supervision. Given that the grouping mechanism is better suited to be learned from more specific instructions rather than general captions, we refrain from incorporating the grouping layer during this phase. Consequently, the pre-training phase follows the same setup as LLaVA [17], where only the image-caption pairs are used to train the image tokenizer.

The key insight here is that, by not introducing the grouping mechanism prematurely, we allow the model to establish a strong foundation in feature alignment between images and language. In this stage, the only trainable parameter is the visual connector W , i.e., $\Theta = W$. This ensures that the visual features extracted from images are properly aligned with the LLM, setting the stage for further fine-tuning in the next phase.

Stage 2: Visual Instruction Tuning Once the image tokenizer has been pre-trained and the visual features are aligned with the language model, we move on to the second stage, which focuses on fine-tuning the model for instruction-aware visual token grouping. At this point, we incorporate the grouping block G along with semantic tokens into the Vision Transformer architecture to enable effective visual token grouping based on specific instructions.

In this stage, we freeze the pre-trained weights of the

visual encoder to retain the feature alignment achieved in Stage 1. However, we continue updating the parameters of the lightweight visual connector W , the grouping layer G , and the LLM ϕ . This means that the trainable parameters during Stage 2 are $\Theta = \{\phi, W, G\}$. Importantly, by introducing the grouping mechanism during instruction-tuning, we ensure that the grouping layer becomes instruction-aware, meaning that the grouping process is directly influenced by the specific instructions provided to the model.

The critical advantage of this approach is that the gradient of the instructions can flow back to the grouping layer, allowing it to learn how to group visual tokens based on the semantics of the instructions rather than solely dependent on the prior knowledge in the vision encoder. This enables the VisToG to achieve a higher level of adaptability and precision when handling visual tasks that require instruction-specific groupings.

4. Experiments

4.1. Datasets

For fair comparison, we conduct experiments on the same datasets as introduced in [17], which is $\sim 558K$ image-text pair for visual connector pre-training and $\sim 665K$ instruction-following data for visual instruction-tuning. Since many image links in the dataset of the instruction tuning stage have expired, compared to the original setting ($\sim 665K$), only $\sim 624K$ data are available. The performance of LLaVA1.5 reported in our analysis is reproduced by ourselves to ensure a fair comparison under the same experimental environment and dataset setting. For downstream tasks, we evaluate our model on GQA [12], TextVQA [21], POPE [14], MMBench [18], ScienceQA [19], MME [10].

4.2. Baselines

We include results of BLIP-2 with Vicuna-13B as LLM backbone, InstructBLIP with Vicuna-7B and Vicuna-13B as LLM backbone, Qwen-VL/Qwen-VL-Chat with Qwen-7B as backbone. These models all adopt Q-Former to conduct the visual token abstraction and hence have a smaller number of image tokens compared with LLaVA (576 tokens). DeCo uses 2D adaptive average pooling to down-sample the visual tokens at the patch level and hence reduce the number of visual tokens to 144. C-Abstractor and D-Abstractor uses convolutional block and deformable attention block to conduct the visual token abstract, also resulting in 144 visual tokens. VoCo-LLaMA compresses the vision tokens using the LLMs as introduced in Sec.2. Here we include the results of 128 tokens for comparison. We also experiment on a very simple yet effective baseline. During inference, we randomly drop the vision tokens from M to M' before feeding into the visual connector. This method is denoted as LLaVA-rand. Besides, to verify effectiveness of

Method	LLM	Res.	#Tokens	IT	GQA	SQA	VQA ^T	POPE	MME	MMB
BLIP-2	Vicuna-13B	224	32	129M	-	61	42.5	85.3	1293.8	-
InstructBLIP	Vicuna-7B	224	64	1.2M	-	60.5	50.1	-	-	36
InstructBLIP	Vicuna-13B	224	64	129M	49.5	63.1	50.7	78.9	1212.8	-
Qwen-VL	Qwen-7B	448	256	1.4B	59.3	67.1	63.8	-	-	38.2
Qwen-VL-Chat	Qwen-7B	448	256	1.4B	57.5	68.2	61.5	-	1487.5	60.6
VoCo-LLaMA	Vicuna-7B	336	128	665K	59.8	-	-	-	-	61.0
DeCo	Vicuna-7B	336	144	665K	54.1	-	56.2	85.9	1373.4	-
C-Abstractor	Vicuna-7B	336	144	665K	52.6	-	55.9	84.5	1411.8	-
D-Abstractor	Vicuna-7B	336	144	665K	53.1	-	55.1	84.6	1313.2	-
LLaVA-1.5	Vicuna-7B	336	576	624K	62.7	70.5	57.3	86.2	1452.0	64.3
LLaVA-1.5-Q-Former	Vicuna-7B	336	576	624K	56.5	70.8	52.2	85.1	1401.0	62.6
LLaVA-1.5-rand	Vicuna-7B	336	144	624K	57.3	70.5	50.4	79.5	1377.0	59.8
LLaVA-1.5 + VisToG	Vicuna-7B	336	128	624K	61.4	70.1	54.5	85.5	1421.2	63.8
LLaVA-1.5 + VisToG	Vicuna-7B	336	64	624K	60.9	70.9	52.5	85.7	1403.7	63.2

Table 1. Performance Comparison with leading methods. VisToG groups the visual tokens into 128 tokens and 64 tokens while achieving highly competitive performance compared with LLaVA. The results of VisToG are highlighted with purple .

Method	#Tokens	GQA	VQA ^T	POPE	MME	Avg
LLaVA-rand	144	91.4	87.9	92.2	94.8	91.6
DeCO	144	86.3	98.0	99.6	94.6	94.6
C-Abstractor	144	83.4	97.5	98.0	97.2	94.0
D-Abstractor	144	84.7	96.1	98.1	90.4	92.4
VisToG	128	97.9	95.1	99.2	97.9	97.5

Table 2. Comparison between Performance Retain Rate (PRT,%) across GQA, TextVQA, POPE, and MME between different methods. The best results are marked as **bold**.

VisToG over Q-Former, we conduct a fair comparison on the LLaVA-v1.5 backbone, but use Q-Former as the connector. The number of queries is set to 64. We denote this method as LLaVA-1.5-QFormer.

4.3. Main results

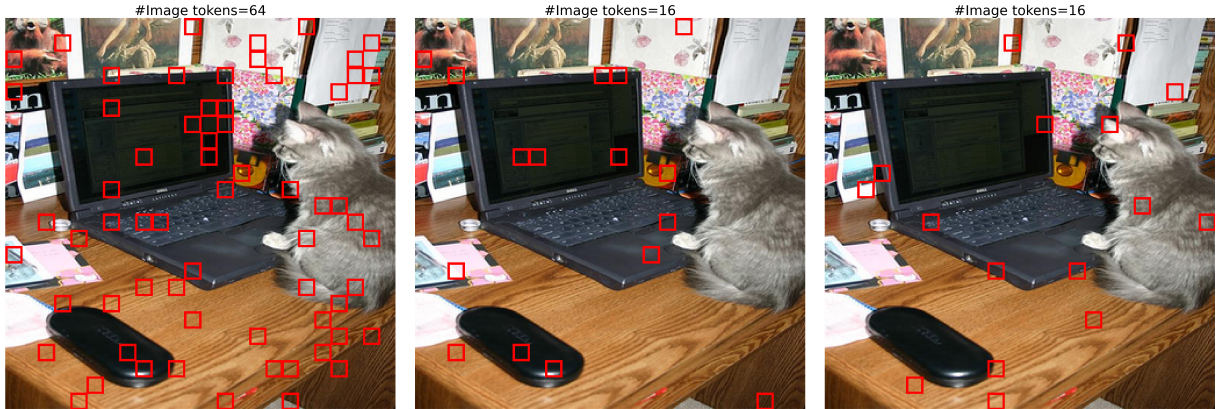
We conduct all experiments on 8×NVIDIA A100-40G and the training configurations are identical to that of LLaVA [17].

From Tab.1 we can identify that LLaVA-rand serves as a considerable baseline. For example, in the 144 image token setting, it beats DeCo, C-Abstractor, and D-Abstractor on GQA dataset and beats DeCo and D-Abstractor on MME dataset. In Fig. 3, we visualize how randomly selected image tokens of LLaVA-rand influence the output of visual question-answering tasks. On the left, we demonstrate that with randomly sampled $N = 64$ image tokens, the MLLM can achieve similar performance compared with LLaVA, which uses $N = 576$ image tokens. This highlights the redundancy inherent in the image tokens and establishes LLaVA-rand as a viable baseline, as further corroborated by the results in Tab.1. As long as the sampled image tokens include those representing critical segments of the image, the performance can be nearly equivalent to that of the original model. This nature also leads to the high variance of the performance of LLaVA-rand. In the middle, we demonstrate

that with randomly sampled $N = 16$ image tokens, the model fails to recognize the presence of a cat. This failure is attributed to the insufficient number of tokens sampled from the cat’s region, underscoring the importance of adequately covering meaningful semantic segments of the image using a limited budget. On the right, with the same number of visual tokens, we manually adjust the distribution of the sampled visual tokens using prior knowledge of the image. By ensuring the tokens are evenly allocated to each significant semantic object within the image, the model can recognize the cat once again. This adjustment demonstrates the importance of token distribution and allocation in achieving better performance, even with a limited number of tokens. More visualization can be found in the Appendix. This motivates our method, if we can automatically sample enough tokens for each important semantic group without a human interface, even with a small number of image tokens we can get considerable results.

The baseline that uses Q-Former with LLaVA-v1.5 backbone falls short in every downstream dataset than VisToG especially in GQA and TextVQA, in which it all witness a performance drop of over five point. This indicate that with the limited amount of data, Q-Former as token compression method is not a good choice. We also include the Performance Retain Rate in Tab. 2. Suppose the downstream datasets are defined by $D = \{D_i\}_{i=1}^{|D|}$, and let the performance of LLaVA with full image tokens on D_i be denoted by b_i . For each model j , let its performance on D_i be denoted by $p_i^{(j)}$. Then the average Performance Retain Rate (PRT) is defined by

$$PRT^{(j)} = \frac{1}{|D|} \sum \frac{p_i^{(j)}}{b_i} \quad (6)$$



(left) The main focus of the image is a cat sitting in front of a laptop computer
 (mid) The main focus of the image is a desk with a computer, which is located in a home office
 (right) The main focus of the image is a cat on a desk in front of a computer.

Figure 3. Visualization of the image tokens selected of the LLaVA-rand. The instruction is "What is the main focus of the image?". Response from LLaVA: "The main focus of the image is a cat sitting on a desk in front of a laptop computer".

4.4. Inference Efficiency

To verify the efficiency of `VisToG`, we conduct experiments on calculating the inference time of different methods. We include the performance of LLaVA-rand as defined before and also re-implement the Adaptive Average Pooling as used in [30], denoted as LLaVA-AvgPool. We calculate the per-sample inference time on different downstream datasets. Let $\{D_i\}_{i=1}^k$ denote the downstream datasets that we aim to infer. For model j , let t_{ij} denote the total inference time on D_i , then average inference time T_j is defined as

$$T_j = \frac{1}{k} \sum_{i=1}^k \frac{t_{ij}}{|D_i|} \quad (7)$$

Since the performance of downstream datasets is in different scales, we calculate the Performance Retain Rate (PRT, %), which is defined as the ratio as compared to the baseline LLaVA that uses all image tokens. As shown in Fig. 2b, the baseline LLaVA that uses all 576 image tokens has an average inference time of 0.15s. As for LLaVA-`VisToG`, it has a significantly higher PRT compared to the LLaVA-rand counterparts while only sacrificing a negligible inference time. While the performance of LLaVA-AvgPool falls between them. All the inference experiments are conducted on a single NVIDIA L40S and are averaged across three runs.

4.5. Ablation Study

4.5.1. Different Attention masks

To verify the effectiveness of the isolated attention, we conduct experiments using the standard full attention of the vision transformer across six downstream datasets. We re-

port the average performance retain rate defined before as the performance metric. As can be seen in Fig.4, we include results of both #tokens=64 and #tokens=128. For both token counts, isolated attention consistently outperforms or matches the performance of full attention across all datasets. Specifically, for #tokens = 64, isolated attention achieves slightly higher performance in GQA, SQA, POPE, MME, and MMB, while showing a notable improvement in TextVQA as well. Similarly, for #tokens = 128, isolated attention continues to demonstrate superior performance in GQA, SQA, POPE, MME, and MMB, with a significant lead in TextVQA. These results suggest that isolated attention is more effective than full attention, particularly in scenarios with varying token counts, making it a more efficient mechanism for multi-modal large language models. The consistent performance advantage of isolated attention across different datasets and token counts underscores its robustness and potential for enhancing the efficiency of multi-modal models.

4.5.2. Number of image tokens

As in Fig. 5, we conduct experiments across varying visual tokens and show the result of `VisToG`, LLaVA-rand and LLaVA-AvgPool on GQA and POPE. As observed in subfigure (a), `VisToG` consistently outperforms LLaVA-rand and LLaVA-AvgPool across all token counts, maintaining relatively high performance even as the number of tokens decreases. LLaVA-AvgPool shows a slight decline in performance but remains relatively stable, whereas LLaVA-rand exhibits a sharp drop when the token count falls below 64. Fig 5 (b) shows a similar trend on the GQA dataset, with `VisToG` again achieving the highest performance across all token counts. LLaVA-AvgPool maintains

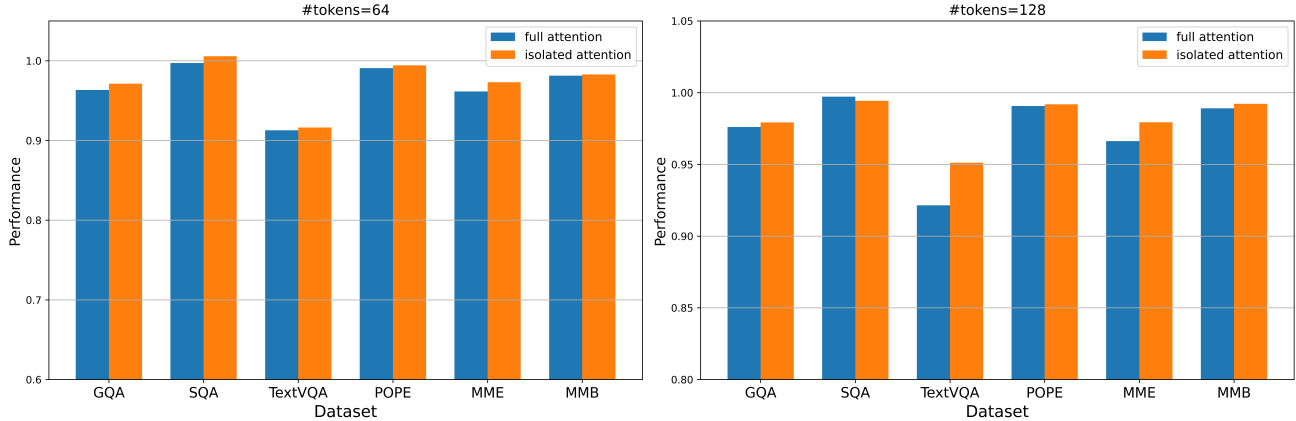


Figure 4. Performance Comparison between standard attention and isolated attention. The numbers are the relative performance compared to the baseline.

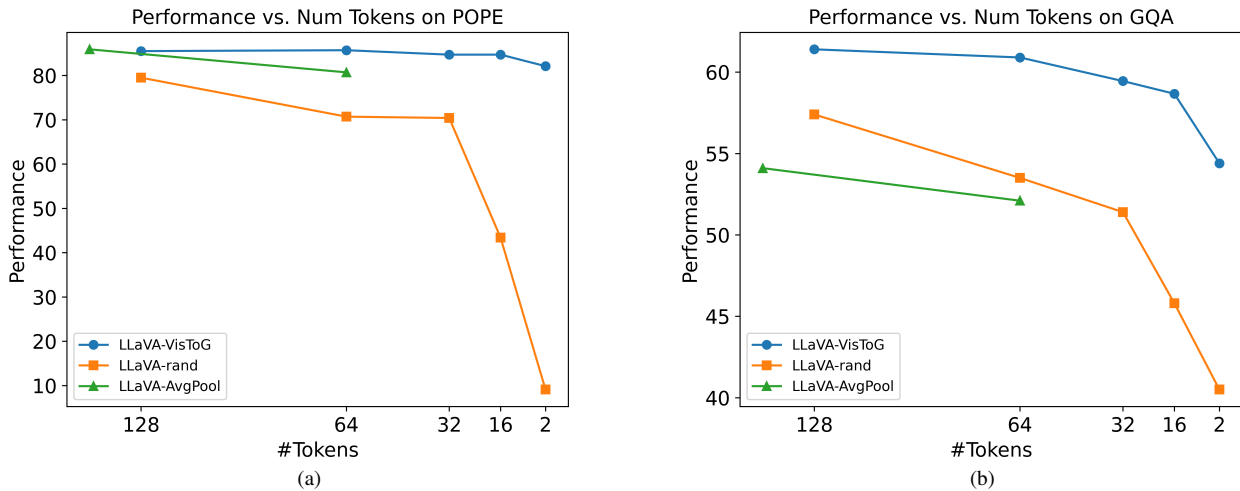


Figure 5. (a) Ablation on the number of image tokens on the POPE dataset. (b) Ablation on the number of image tokens on GQA dataset.

a moderate performance level, while LLaVA-rand experiences a significant degradation in performance as the token count decreases, particularly when reduced to 32 tokens or fewer. These results suggest that VisToG is the most robust method in handling reduced token counts, while LLaVA-rand is highly sensitive to token reduction, indicating the randomness causes loss of visual information when the visual tokens are very limited.

5. Conclusion and Discussions

In this paper, we have introduced VisToG, a novel grouping mechanism designed to address the substantial computational costs associated with Multi-modal Large Language Models (MLLMs). By leveraging pre-trained vision encoders to group similar image segments without the need for additional segmentation masks, VisToG effectively re-

duces inference costs. Our approach utilizes isolated attention to identify and eliminate redundant visual tokens, significantly decreasing computational demands. Extensive experiments validate the efficacy of VisToG, demonstrating that it maintains 98.1% of the original performance while achieving a reduction of over 27% in inference time. This advancement enhances the efficiency of MLLMs and provides insights on training larger MLLMs with minimal image token redundancies.

Limitation and Future work Due to resource limits, we didn't conduct experiments on video setting. But VisToG can be easily adapted to other frameworks for efficient MLLM inference. Future research could focus on extending the application of VisToG to video-based scenarios, thereby verifying its effectiveness when processing dynamic and temporal data.

References

- [1] Josh Achiam, Steven Adler, Sandhini Agarwal, Lama Ahmad, Ilge Akkaya, Florencia Leoni Aleman, Diogo Almeida, Janko Altenschmidt, Sam Altman, Shyamal Anadkat, et al. Gpt-4 technical report. *arXiv preprint arXiv:2303.08774*, 2023. 1
- [2] Jinze Bai, Shuai Bai, Yunfei Chu, Zeyu Cui, Kai Dang, Xiaodong Deng, Yang Fan, Wenbin Ge, Yu Han, Fei Huang, et al. Qwen technical report. *arXiv preprint arXiv:2309.16609*, 2023. 1, 2
- [3] James Betker, Gabriel Goh, Li Jing, Tim Brooks, Jianfeng Wang, Linjie Li, Long Ouyang, Juntang Zhuang, Joyce Lee, Yufei Guo, et al. Improving image generation with better captions. *Computer Science*. <https://cdn.openai.com/papers/dall-e-3.pdf>, 2(3):8, 2023. 2
- [4] Daniel Bolya, Cheng-Yang Fu, Xiaoliang Dai, Peizhao Zhang, Christoph Feichtenhofer, and Judy Hoffman. Token merging: Your vit but faster. *arXiv preprint arXiv:2210.09461*, 2022. 3
- [5] Junbum Cha, Wooyoung Kang, Jonghwan Mun, and Byungseok Roh. Honeybee: Locality-enhanced projector for multimodal llm. In *Proceedings of the IEEE/CVF Conference on Computer Vision and Pattern Recognition*, pages 13817–13827, 2024. 1, 3
- [6] Wenhao Chai, Enxin Song, Yilun Du, Chenlin Meng, Vashisht Madhavan, Omer Bar-Tal, Jeng-Neng Hwang, Saining Xie, and Christopher D Manning. Auroracap: Efficient, performant video detailed captioning and a new benchmark. *arXiv preprint arXiv:2410.03051*, 2024. 3
- [7] Liang Chen, Haozhe Zhao, Tianyu Liu, Shuai Bai, Junyang Lin, Chang Zhou, and Baobao Chang. An image is worth 1/2 tokens after layer 2: Plug-and-play inference acceleration for large vision-language models. *arXiv preprint arXiv:2403.06764*, 2024. 1
- [8] Wei-Lin Chiang, Zhuohan Li, Zi Lin, Ying Sheng, Zhanghao Wu, Hao Zhang, Lianmin Zheng, Siyuan Zhuang, Yonghao Zhuang, Joseph E Gonzalez, et al. Vicuna: An open-source chatbot impressing gpt-4 with 90%* chatgpt quality. See <https://vicuna.lmsys.org> (accessed 14 April 2023), 2(3):6, 2023. 1
- [9] Wenliang Dai, Junnan Li, Dongxu Li, Anthony Meng Huat Tiong, Junqi Zhao, Weisheng Wang, Boyang Li, Pascale Fung, and Steven C. H. Hoi. Instructblip: Towards general-purpose vision-language models with instruction tuning. In *Advances in Neural Information Processing Systems 36: Annual Conference on Neural Information Processing Systems 2023, NeurIPS 2023, New Orleans, LA, USA, December 10 - 16, 2023*, 2023. 2
- [10] Chaoyou Fu, Peixian Chen, Yunhang Shen, Yulei Qin, Mengdan Zhang, Xu Lin, Zhenyu Qiu, Wei Lin, Jinrui Yang, Xiawu Zheng, Ke Li, Xing Sun, and Rongrong Ji. MME: A comprehensive evaluation benchmark for multimodal large language models. *CoRR*, abs/2306.13394, 2023. 5
- [11] Suyu Ge, Yunan Zhang, Liyuan Liu, Minjia Zhang, Jiawei Han, and Jianfeng Gao. Model tells you what to discard: Adaptive kv cache compression for llms. *arXiv preprint arXiv:2310.01801*, 2023. 3
- [12] Drew A Hudson and Christopher D Manning. Gqa: A new dataset for real-world visual reasoning and compositional question answering. In *Proceedings of the IEEE/CVF conference on computer vision and pattern recognition*, pages 6700–6709, 2019. 5
- [13] Junnan Li, Dongxu Li, Silvio Savarese, and Steven Hoi. Blip-2: Bootstrapping language-image pre-training with frozen image encoders and large language models. In *International conference on machine learning*, pages 19730–19742. PMLR, 2023. 2, 3
- [14] Yifan Li, Yifan Du, Kun Zhou, Jinpeng Wang, Wayne Xin Zhao, and Ji-Rong Wen. Evaluating object hallucination in large vision-language models. *arXiv preprint arXiv:2305.10355*, 2023. 5
- [15] Zhimin Li, Jianwei Zhang, Qin Lin, Jiangfeng Xiong, Yanxin Long, Xincheng Deng, Yingfang Zhang, Xingchao Liu, Minbin Huang, Zedong Xiao, et al. Hunyuan-dit: A powerful multi-resolution diffusion transformer with fine-grained chinese understanding. *arXiv preprint arXiv:2405.08748*, 2024. 2
- [16] Bin Lin, Zhenyu Tang, Yang Ye, Jiayi Cui, Bin Zhu, Peng Jin, Junwu Zhang, Munan Ning, and Li Yuan. Moe-llava: Mixture of experts for large vision-language models. *arXiv preprint arXiv:2401.15947*, 2024. 3
- [17] Haotian Liu, Chunyuan Li, Qingyang Wu, and Yong Jae Lee. Visual instruction tuning. *Advances in neural information processing systems*, 36, 2024. 1, 3, 5, 6
- [18] Yuan Liu, Haodong Duan, Yuanhan Zhang, Bo Li, Songyang Zhang, Wangbo Zhao, Yike Yuan, Jiaqi Wang, Conghui He, Ziwei Liu, et al. Mmbench: Is your multi-modal model an all-around player? *arXiv preprint arXiv:2307.06281*, 2023. 5
- [19] Pan Lu, Swaroop Mishra, Tanglin Xia, Liang Qiu, Kai-Wei Chang, Song-Chun Zhu, Oyvind Tafjord, Peter Clark, and Ashwin Kalyan. Learn to explain: Multimodal reasoning via thought chains for science question answering. *Advances in Neural Information Processing Systems*, 35:2507–2521, 2022. 5
- [20] Alec Radford, Jong Wook Kim, Chris Hallacy, Aditya Ramesh, Gabriel Goh, Sandhini Agarwal, Girish Sastry, Amanda Askell, Pamela Mishkin, Jack Clark, et al. Learning transferable visual models from natural language supervision. In *International conference on machine learning*, pages 8748–8763. PMLR, 2021. 1, 3
- [21] Amanpreet Singh, Vivek Natarajan, Meet Shah, Yu Jiang, Xinlei Chen, Dhruv Batra, Devi Parikh, and Marcus Rohrbach. Towards vqa models that can read. In *Proceedings of the IEEE/CVF conference on computer vision and pattern recognition*, pages 8317–8326, 2019. 5
- [22] Shengbang Tong, Ellis Brown, Penghao Wu, Sanghyun Woo, Manoj Middepogu, Sai Charitha Akula, Jihan Yang, Shusheng Yang, Adithya Iyer, Xichen Pan, et al. Cambrian-1: A fully open, vision-centric exploration of multimodal llms. *arXiv preprint arXiv:2406.16860*, 2024. 3
- [23] Shengbang Tong, Zhuang Liu, Yuexiang Zhai, Yi Ma, Yann LeCun, and Saining Xie. Eyes wide shut? exploring the visual shortcomings of multimodal llms. In *Proceedings of*

- the IEEE/CVF Conference on Computer Vision and Pattern Recognition*, pages 9568–9578, 2024. 3
- [24] Hugo Touvron, Louis Martin, Kevin Stone, Peter Albert, Amjad Almahairi, Yasmine Babaei, Nikolay Bashlykov, Soumya Batra, Prajjwal Bhargava, Shruti Bhosale, et al. Llama 2: Open foundation and fine-tuned chat models. *arXiv preprint arXiv:2307.09288*, 2023. 1
- [25] Aaron Van Den Oord, Oriol Vinyals, et al. Neural discrete representation learning. *Advances in neural information processing systems*, 30, 2017. 4
- [26] Haonan Wang, Minbin Huang, Runhui Huang, Lanqing Hong, Hang Xu, Tianyang Hu, Xiaodan Liang, Zhenguo Li, Hong Cheng, and Kenji Kawaguchi. Boosting visual-language models by exploiting hard samples. *arXiv preprint arXiv:2305.05208*, 2023. 3
- [27] Guangxuan Xiao, Yuandong Tian, Beidi Chen, Song Han, and Mike Lewis. Efficient streaming language models with attention sinks. *arXiv preprint arXiv:2309.17453*, 2023. 3
- [28] Jiarui Xu, Shalini De Mello, Sifei Liu, Wonmin Byeon, Thomas Breuel, Jan Kautz, and Xiaolong Wang. Groupvit: Semantic segmentation emerges from text supervision. In *Proceedings of the IEEE/CVF Conference on Computer Vision and Pattern Recognition*, pages 18134–18144, 2022. 4
- [29] Zhengyuan Yang, Linjie Li, Kevin Lin, Jianfeng Wang, Chung-Ching Lin, Zicheng Liu, and Lijuan Wang. The dawn of lmms: Preliminary explorations with gpt-4v (ision). *arXiv preprint arXiv:2309.17421*, 9(1):1, 2023. 2
- [30] Linli Yao, Lei Li, Shuhuai Ren, Lean Wang, Yuanxin Liu, Xu Sun, and Lu Hou. Deco: Decoupling token compression from semantic abstraction in multimodal large language models. *arXiv preprint arXiv:2405.20985*, 2024. 1, 3, 7
- [31] Xubing Ye, Yukang Gan, Xiaoke Huang, Yixiao Ge, Ying Shan, and Yansong Tang. Voco-llama: Towards vision compression with large language models. *arXiv preprint arXiv:2406.12275*, 2024. 3
- [32] Zhengqing Yuan, Zhaoxu Li, and Lichao Sun. Tinygpt-v: Efficient multimodal large language model via small backbones. *arXiv preprint arXiv:2312.16862*, 2023. 3
- [33] Xiaohua Zhai, Basil Mustafa, Alexander Kolesnikov, and Lucas Beyer. Sigmoid loss for language image pre-training. In *Proceedings of the IEEE/CVF International Conference on Computer Vision*, pages 11975–11986, 2023. 3
- [34] Pan Zhang, Xiaoyi Dong, Yuhang Zang, Yuhang Cao, Rui Qian, Lin Chen, Qipeng Guo, Haodong Duan, Bin Wang, Linke Ouyang, et al. Internlm-xcomposer-2.5: A versatile large vision language model supporting long-contextual input and output. *arXiv preprint arXiv:2407.03320*, 2024. 2, 3
- [35] Baichuan Zhou, Ying Hu, Xi Weng, Junlong Jia, Jie Luo, Xien Liu, Ji Wu, and Lei Huang. Tinyllava: A framework of small-scale large multimodal models. *arXiv preprint arXiv:2402.14289*, 2024. 3
- [36] Deyao Zhu, Jun Chen, Xiaoqian Shen, Xiang Li, and Mohamed Elhoseiny. Minigpt-4: Enhancing vision-language understanding with advanced large language models. *arXiv preprint arXiv:2304.10592*, 2023. 1, 3